Received: 28 August 2019 | Revised: 19 March 2020 | Accepted: 14 April 2020

DOI: 10.1111/psyp.13594

Check for updates

ORIGINAL ARTICLE

PSYCHOPHYSIOLOGY SPR WILEY

Neural correlates of fluctuations in the intermediate band for heart rate and respiration are related to interoceptive perception

Micha Keller[1] | **Holger Pelz**[2] | **Volker Perlitz**[3] | **Jana Zweerings**[1] | **Erik Röcher**[1] | **Halim Ibrahim Baqapuri**[1] | **Klaus Mathiak**[1,4]

[1]Department of Psychiatry, Psychotherapy and Psychosomatics, Medical School, RWTH Aachen University, Aachen, Germany

[2]Deutsche Gesellschaft für Osteopathische Medizin (DGOM), Mannheim, Germany

[3]Simplana GmbH, Aachen, Germany

[4]Jülich Aachen Research Alliance (JARA), Translational Brain Medicine, Jülich, Germany

Correspondence
Micha Keller, Department of Psychiatry, Psychotherapy and Psychosomatics, Medical School, RWTH Aachen University, Pauwelsstraße 30, Aachen, 52074, Germany.
Email: mkeller@ukaachen.de

Funding information
HEAD-Genuit Foundation; German Ministry for Education and Research, Grant/Award Number: 01EE1405A-C; German Research Foundation, Grant/Award Number: IRTG 2150; RWTH Aachen University

Abstract

Supratentorial brain structures such as the insula and the cingulate cortex modulate the autonomic nervous system (ANS). The neural underpinnings of separate frequency bands for variability in cardiac and respiratory data have been suggested in explaining parasympathetic and sympathetic ANS modulation. As an extension, an intermediate (IM) band in peripheral physiology has been considered to reflect psychophysiological states during rest. Using functional magnetic resonance imaging (fMRI), we investigated the neural correlates associated with IM band variability in cardiac and respiratory rate and identified dissociable networks for LF, IM, and HF bands in both modalities. Cardiac and respiratory IM band fluctuations correlated with blood oxygen level-dependent (BOLD) signal in the mid and posterior insula and the secondary somatosensory area, that is, regions related to interoceptive perception. These data suggest that in addition to the commonly considered LF and HF bands, other frequency components represent relevant physiological constituents. The IM band may be instrumental for assessment of the CNS-ANS interaction. In particular, the relation between the IM band and interoception may be of physiological and clinical interest.

KEYWORDS

autonomic regulation, depression, osteopathy, psychiatry, resting-state fMRI

1 | INTRODUCTION

The autonomic nervous system (ANS) receives modulatory input from high-level supra-tentorial brain structures, which affects peripheral physiological measures such as heart rate variability (HRV), respiration, and electrodermal activity (see Beissner, Meissner, Bär, & Napadow, 2013 for a meta-analysis). For instance, in the neurovisceral integration model for HRV (Thayer & Lane, 2009), neocortical areas such as the prefrontal and cingulate cortex exert tonic inhibitory control over brainstem circuitry underlying the ANS regulation. A similar cortico-limbic model has been proposed for sensorimotor integration of respiration (Evans, 2010), with an interplay of volitional respiratory control (pre-motor and supplementary motor area (SMA)) and interoceptive integration areas (anterior cingulate cortex (ACC), insula, and amygdala). These models overlap in core autonomic network areas, including the cingulate cortex, insula, and amygdala

This is an open access article under the terms of the Creative Commons Attribution-NonCommercial-NoDerivs License, which permits use and distribution in any medium, provided the original work is properly cited, the use is non-commercial and no modifications or adaptations are made.
© 2020 The Authors. Psychophysiology published by Wiley Periodicals LLC on behalf of Society for Psychophysiological Research

(see also Beissner et al., 2013). However, there is no consensus over an integrative model for heart rate and respiration regulation.

Sympathetic and parasympathetic regulation of the ANS acts differently across frequency bands. Conventionally, HRV is separated into the low-frequency (LF; 0.04–0.15 Hz) and high-frequency bands (HF; 0.15–0.4 Hz). However, there are inconsistent definitions of the boundaries proposed for HRV bands describing cardiac ANS regulation (Kettunen & Keltikangas-Järvinen, 2001). HF-HRV reflects respiratory sinus arrhythmia and increases with elevated parasympathetic vagal tone. In contrast, LF-HRV is related to both sympathetic and parasympathetic neural activity. Besides a dominant parasympathetic contribution, it is suggested that it captures its own physiological mechanism (e.g., Reyes del Paso, Langewitz, Mulder, Van Roon, & Duschek, 2013). Another line of research suggested that the LF band represents subharmonics of a central pacemaker in the lower brainstem region (Perlitz, Cotuk, Lambertz, et al., 2004). Respiration, on the contrary, seems to largely modulate RSA/HF-HRV and control over its rate and depth are often advocated (Ritz & Dahme, 2006). However, variability of respiration in separate frequency bands has been shown sensitive to cognitive workload (Hidalgo-Muñoz et al., 2018; Veltman & Gaillard, 1996). Furthermore, respiration pattern variability could be used as an indicator of emotional processing (Zamoscik et al., 2018). Interestingly, changes in the functional connectivity relate to main peak frequency of breathing in MRI measurements and persist even when correcting for physiological noise. Thus, the covariation between the peripheral physiology and the blood oxygen level-dependent (BOLD) signal implies physiological functions (Birn, 2012). However, studies investigating BOLD signals of respiratory parameters are needed to further clarify their neurophysiological underpinnings. In addition, different ANS target modalities and alternate definitions of the frequency bands must be considered.

Neural correlates of parasympathetic and sympathetic changes have been extensively described for the LF and HF bands. However, several studies indicate blood flow oscillations around the 0.15-Hz mark depending on physiological states (Smits, Aarnoudse, Geerdink, & Zijlstra, 1987; Ziege, Schmid-Schönbein, Grebe, & Martin, 1997). Subsequently, these observations led to the introduction of the intermediate (IM) band that was systematically investigated by Perlitz, Lambertz, et al. (2004). In particular, power in the IM band increased when experts practiced autogenic relaxation training (AT) and also increased during the subjective feeling of relaxation in subjects untrained in this relaxation technique (Perlitz, Cotuk, Schiepek, et al., 2004). Furthermore, the presence of the IM band in the heart rate for extended periods during psychomotor relaxation was associated with cardiorespiratory phase synchronizations (CRPS) (Perlitz, Lambertz, et al., 2004). Other studies found significant differences in IM band activity in response to individually chosen or standardized relaxation music (Ernst & Petzold, 2012). In contrast, IM band activity has been shown to disappear due to cold pressor-induced pain (Krautstrunk & Schmid-Schönbein, 2008; Lampmann & Petzold, 2006). Furthermore, the IM band can be inhibited by atropine infusion, and therefore, was related to parasympathetic facilitation (Podgoreanu, Stout, El-Moalem, & Silverman, 2002; Silverman & Stout, 2002; Silverman, Stout, Lee, & Ferneini, 2001). CRPS, as observed in the IM band, appeared to be independent from modulation by the respiratory influences and the baroreceptor reflexes (Perlitz, Cotuk, Lambertz, et al., 2004). Further, IM activity was independent from baroreflex related 0.1-Hz waves, as both rhythms persisted in parallel despite cardiovascular-respiratory resonance at 0.15 or 0.1 Hz (Perlitz, Lambertz, et al., 2004). Therefore, CRPS signifies a phenomenon of physiological relevance, which has only recently attracted new scientific attention (Scholkmann & Wolf, 2019).

The IM band seems to be central for brain-heart interactions (see recent review by Schwerdtfeger et al., 2019). Preliminary evidence suggests that 0.15 Hz waves originate in the brain stem and travel to skin microvasculature through parasympathetic nerves (Perlitz, Cotuk, Lambertz, et al., 2004). One interpretation of this phenomenon is that it yields an energetic benefit over chaotic states (Toledo, Akselrod, Pinhas, & Aravot, 2002). This may also hold for the increase in IM band activation and synchronization of various physiological parameters, which appear to offer information about transitions from states of physiological arousal to states of relaxation (e.g., AT).

Despite a considerable number of studies on the IM band, investigations of neural correlates of IM band activity in humans are still missing and its physiological mechanism and relevance remain poorly understood. Initial evidence on the neural mechanism of the IM band comes from animal studies, which demonstrated strikingly similar rhythms originating in the reticular formation of the brainstem (Lambertz & Langhorst, 1998; Langhorst, Lambertz, & Schulz, 1986). In these studies, the application of anesthetics was associated with a general decline of basic activity and a concurrent emergence of the IM band in the reticular formation, coupling with other physiological signals (e.g., Lambertz, Vandenhouten, Grebe, & Langhorst, 2000). However, to further support the translational value of these results, studies of the neural correlates of the IM band in humans are needed.

The goal of this study is an analysis of the neural correlates of the IM band in cardiac and respiratory data, which may possibly be involved in a top-down regulation of subcortical and brainstem cardiorespiratory regulatory areas during resting state (RS) fMRI. First, we expect fluctuations of the IM band in cardiac and respiratory data to correlate with brain

activity changes in core ANS regulation centers such as the ACC, the middle cingulate cortex (MCC), the amygdala, and the periaqueductal grey (PAG). Second, based on the clear distinction of the IM band and other frequency bands (Perlitz, Lambertz, et al., 2004), we expect the brain activity patterns in the IM band to differ from those of the LF and HF bands.

2 | METHOD

2.1 | Participants

Forty-one right-handed, healthy adults (17 women, age 30.9 ± 9.9 years) volunteered for this study. Participants had an average body mass index (BMI) of 23.6 ± 3.25 kg/m^2 and normal blood pressure status. Four participants reported to smoke on a regular basis (10–20 cigarettes/day). Exclusion criteria were contraindications for MR, self-reported neurological or psychiatric disorders as well as the current use of any psychoactive medications. Recruitment was conducted through advertisements within the university hospital Aachen. The experiment was conducted according to the Code of Ethics of the World Medical Association (Williams, 2008). All subjects provided written, informed consent, and all protocols were approved by the Institutional Review Board of the medical faculty (EK 050/17).

2.2 | Procedure

Recording of RS fMRI data was conducted at the beginning (Rest1) and the end (Rest2) of a neurofeedback (NF) training session on two separate days. NF methodology is used to train self-regulation of circumscribed brain areas with real-time fMRI and assess their behavioral effects (Weiskopf et al., 2003). However, no specific hypothesis considered NF associated changes. During RS sessions, participants did not perform any intentional task and were instructed to look at a white fixation cross on a black screen, to keep their eyes open, to remain awake, and to let their thoughts freely wander during the scan. Studies have shown differences in connectivity for eyes open versus eyes closed (e.g., Agcaoglu, Wilson, Wang, Stephen, & Calhoun, 2019), but have not reported one condition being definitely superior to the other. We chose the eyes open condition in order to minimize the risk of participants falling asleep during the long fMRI scanning sessions. Furthermore, the eyes open condition is also used by big imaging consortia such as the human connectome project (Smith et al., 2013). Each RS session lasted 480 s. Structural images were acquired on a separate day prior to these measurements. Smokers could smoke before the fMRI measurements in order to prevent withdrawal symptoms during measurements.

2.2.1 | fMRI data acquisition

Images were acquired by a 3T Siemens Magnetom Prisma whole-body MRI scanner (Siemens Medical) using a standard 20-channel head coil. For structural registration and normalization, a T1-weighted anatomical scan using an MPRAGE sequence (FOV = 256 × 256 mm, 176 sagittal slices, 1-mm^3 isotropic voxels, TR = 2,000 ms, TI = 900 ms, TE = 3.03 ms, flip angle = 9°) was acquired from every participant. RS fMRI series of 240 volumes each were recorded using an echo-planar imaging (EPI) sequence (TE = 28 ms, TR = 2,000 ms, flip angle = 77°, voxel size = 3 × 3 × 3 mm^3, matrix size = 64 × 64, 34 transversal slices with 0.75-mm gap).

2.2.2 | Cardiorespiratory data acquisition

Heart rate as well as respiration were recorded concurrently with MRI using the MR-compatible BIOPAC MP150 system (Biopac Systems Inc., USA). Data were continuously recorded at 2,000 samples/s with a photoplethysmograph (PPG) placed on the index finger of the left hand and a pneumatic respiratory belt strapped around the participant's abdomen. For synchronization with the imaging data, trigger pulses, indicating the beginning of functional MRI volumes, were recorded. Despite the higher temporal precision of ECG, PPG was chosen over the electrical recordings as it is less likely to be corrupted by MR-gradient artefacts. Furthermore, PPG- and ECG-derived HRV measures correlated highly during rest despite some findings of overestimated short-term indices such as RMSSD or HF during physical strain (Schäfer & Vagedes, 2013). In specific, power spectra of PPG and ECG-derived tachograms have been found to be functionally similar in LF and HF bands (Selvaraj, Jaryal, Santhosh, Deepak, & Anand, 2008). Nevertheless, the equivalence of PPG and ECG activity in the IM band still need to be confirmed in particular with respect to hemodynamic phenomena such as Mayer waves (Yücel et al., 2016).

2.3 | Data analysis

From the PPG and the respiratory belt signal, heart and respiration cycles as well as rates were extracted. Using spectrographic time frequency analysis, energy in different frequency bands were extracted. These values were combined into instantaneous measures for the TR = 2 s intervals. The predictors of interest for the BOLD signal were delayed to account for the hemodynamic response and entered a general linear model for the RS fMRI signal. Figure 1 gives an overview of the data analysis steps, which are detailed in the following subsections.

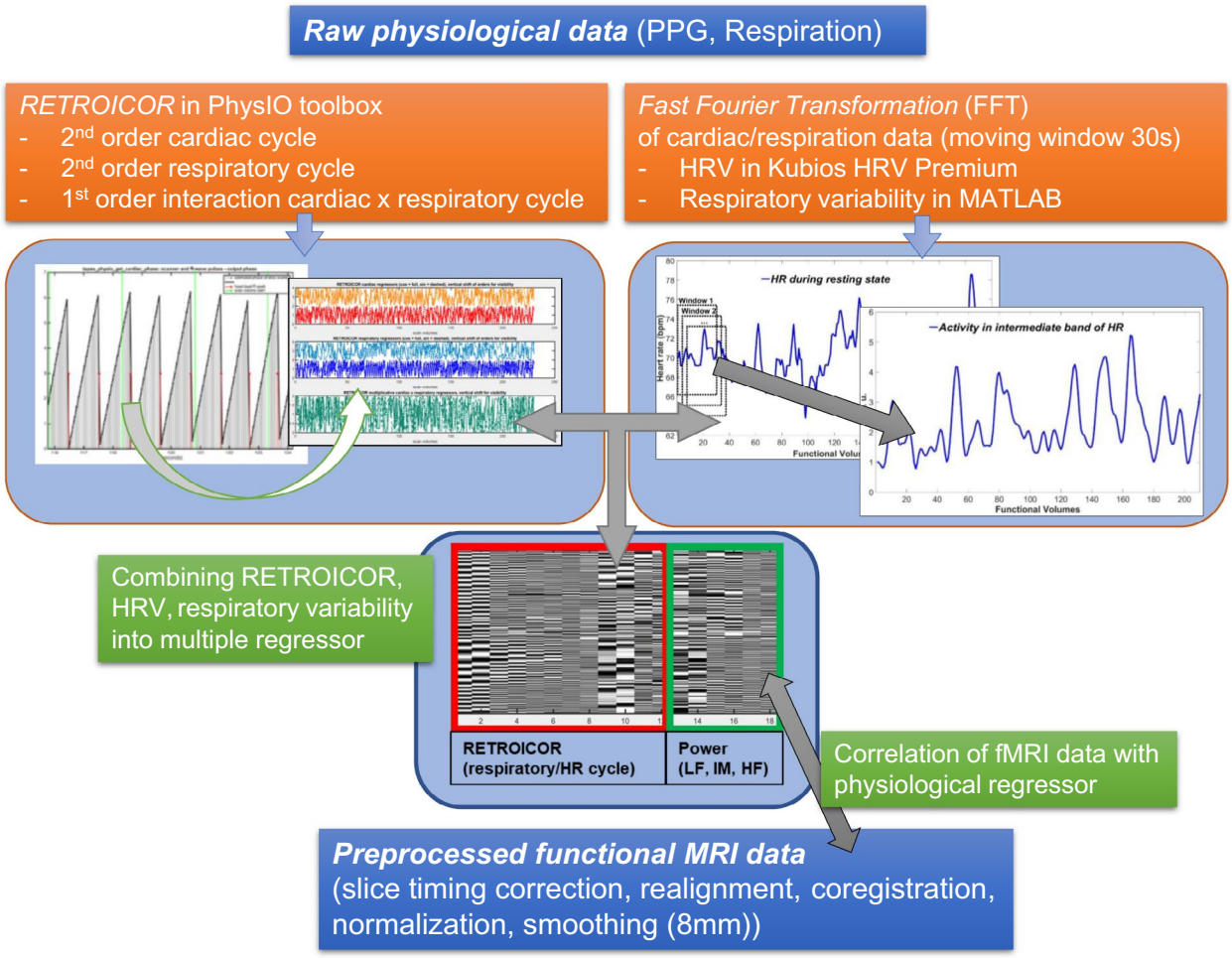

FIGURE 1 Analysis pipeline of peripheral physiological data. Physiological regressors were created containing predictors for physiological noise (RETROCOIR; cardiac and respiratory cycle and their interaction) as well as power in the LF (0.05–0.12 Hz), IM (0.12–0.18 Hz), and HF (0.18–0.4 Hz) bands. Multiple regressors then entered the GLM for the mapping analysis of the preprocessed fMRI data

2.3.1 | Cardiorespiratory data analysis

The data segments recorded simultaneously during the resting state sessions were extracted for further processing in the HRV analysis software Kubios HRV Premium (version 3.1, Kuopio, Finland) and a customized version of the PhysIO Toolbox (version 2.6.0, Kasper et al., 2017). Data were used only if physiological data were complete and did not exhibit intervals of signal loss due to, for example, hand movement in either of the RS sessions of a day. Six pairs of RS sessions were excluded due to poor signal quality. The automatic artifact correction of Kubios was applied to the PPG signal leading to 0.63% ± 0.57% corrected events for HRV analysis. In few cases, missed heart beats were corrected manually whenever the correct time point could be clearly identified.

Frequency bands were defined as LF (0.05–0.12 Hz), IM (0.12–0.18 Hz), and HF (0.18–0.40 Hz). This classification incorporates the current literature on HRV, in which frequencies are usually defined as low and high (Camm et al., 1996; Shaffer & Ginsberg, 2017), as well as the IM band (e.g., Perlitz, Cotuk, Lambertz, et al., 2004). In addition, this split is in accordance with the power spectrum of cardiac and respiratory data, which reveal large variation within the three frequency bands across the participants (Appendix A). Frequency- and time-domain HRV and respiration measures were extracted for the defined frequencies with Kubios for HRV and the MATLAB spectrogram function for respiration. HRV power data were logarithmically transformed to reduce skewness. Similarly, a Box-Cox transformation ($\lambda = 0.05$) was applied to the power of the respiratory bands. Repeated measures analyses of covariance (rmANCOVAs) examined the mean power in the specified frequency bands (LF, IM, and HF) in HRV and respiration, during each RS measurement (pre and post NF) with age and gender as covariates. Changes of absolute cardiac and respiratory values (pre to post NF) were further investigated by two-sided paired t tests. Furthermore, to investigate the (transmodal) interaction between the three frequency bands, a 3×3 repeated-measures analysis of variance (rmANOVA) of the correlations between cardiac and respiratory power with factor "HRV" (LF, IM, HF) and factor "respiration" (LF, IM,

HF) was computed. Statistical analyses were performed with Statistical Package for the Social Sciences (SPSS), version 25.0 (SPSS Inc., Chicago, IL, USA). A p-value of $< .05$ was considered statistically significant.

For the correlation between physiological signal variations over time and the BOLD signal, power values in specified frequency bands were computed for each functional volume using a moving window of 15 volumes (30 s). The trade-off between temporal and frequency resolution complicates the choice of time window duration. The 30 s time window was chosen as it covers all important frequencies (frequency resolution = 0.033 Hz) while preserving an acceptable temporal resolution. For each window, a fast Fourier transformation (FFT) was performed. Time-shifted power values for the LF (0.05–0.12 Hz), IM (0.12–0.18 Hz), and HF (0.18–0.4 Hz) of HRV and respiration parameters served as predictors in the fMRI first-level model.

2.3.2 | fMRI data preprocessing

To ensure high quality functional and structural MRI data, all data sets were examined within 48 hr following recording using a standardized quality assurance pipeline developed and used by the Psychiatric Imaging Network Germany (PING; ping-rwth-aachen.de). This entailed the assessment of functional data within the Automated Quality Assurance toolbox (AQuA; Stöcker et al., 2005). All fMRI data used for further analyses had percent signal change values below 4. Quality of structural data was assured by the quality parameters of the Computational Anatomy Toolbox (CAT; Gaser & Dahnke, 2016).

fMRI data were preprocessed in Matlab (Mathworks Inc., Natick, MA) using the Statistical Parametric Mapping 12 toolbox (SPM12; https://www.fil.ion.ucl.ac.uk/spm/software/spm12/). To minimize T1-saturation effects, the first five volumes of each RS session were discarded for data analysis. Functional fMRI data were corrected for slice-timing and realigned to the first volume (6 movement parameters). Furthermore, fMRI data were co-registered to the participant's structural T1 image, smoothed with an 8 mm FWHM Gaussian kernel and normalized to the T1-weighted ICBM152 brain template of the Montreal Neurological Institute (MNI). Data from all participants were visually inspected after preprocessing to ensure adequate coregistration and normalization. Movement parameters did not exceed 3 mm within any resting state scan. For the reduction of cardiac and respiratory artefacts, RETROICOR phase expansion was performed using 2nd order cardiac and respiratory phases as well as the 1st order cardiac and respiratory interaction, yielding 12 parameters (Glover, Li, & Ress, 2000; implementation in PhysIO Toolbox, Kasper et al., 2017). To improve peak detection for cardiac data, a custom modification of the PhysIO toolbox filtered out slow baseline signal fluctuations and noise using a 4th order bandpass filter (0.5–30 Hz).

2.3.3 | fMRI data analysis

Brain mapping analysis was performed using SPM12. The 12 RETROICOR regressors for physiological noise reduction as well as the LF, IM, and HF power in cardiac and respiratory variation were entered into the first-level GLM analysis of fMRI RS data. In detail, the 18 parameters were:

1–4	*RETROICOR—cardiac cycle up to 2nd order expansion*
5–8	*RETROICOR—respiratory cycle up to 2nd order expansion*
9–12	*RETROICOR—heart-respiration interaction up to 1st order expansion*
13–15	*Power in HRV frequency bands (LF, IM, and HF)*
16–18	*Power in respiration in LF, IM, and HF bands*

To investigate the neural networks underlying ANS regulation, the power time-series of heart rate and respiration were shifted backward in time by 5 s to account for the hemodynamic delay. In contrast, the cardiac and respiratory cycles were considered to elicit artifactual signal fluctuations without neurovascular coupling. On the group level, two distinct 2×3 (pre vs. post × LF vs. IM vs. HF) rmANOVAs were computed for cardiac and respiratory variability each. Further, age, BMI and smoking status were included as covariates of no interest. Across the gray matter mask, a voxel-wise threshold of $p < .001$ was applied and family-wise error (FWE) correction of $p_{FWE} < .05$) was applied at cluster level.

2.3.4 | Region of interest (ROI) analysis

An exploratory ROI analysis investigated contributions of specific frequency bands on brain activation. The anatomical ROI selection was based on the meta-analysis by Beissner et al. (2013) of neural correlates of autonomic regulation. Core areas for autonomic regulation selected for ROI analysis were the ACC, MCC, PCC, amygdaloid complex (amygdala combined with hippocampal formation), (infra-) parietal areas (supramarginal and angular gyri), and insula (see Beissner et al., 2013). Furthermore, a somatosensorimotor network was chosen as a ROI due to its importance in AT (e.g., Schlamann, Naglatzki, de Greiff, Forsting, & Gizewski, 2010). The ROI masks were created using the Automated Anatomical Labeling atlas in the SPM WFU PickAtlas toolbox (v 3.0.5; Maldjian, Laurienti, Kraft, & Burdette, 2003) and dimensions adjusted according to their anatomical extent (ACC: 2,701 voxels; MCC: 4,144 voxels; PCC: 10,560 voxels; Amygdala: 1,718 voxels; PAG: 1,773 voxels; Parietal: 5,052 voxels; Sensorimotor: 18,570 voxels; Insula: 3,462 voxels). For the somatosensorimotor network

ROI, the parietal operculum divisions (OP1–4) and secondary somatosensory cortex (SS2) ROIs were taken from the SPM Anatomy Toolbox (version 2.2c; Eickhoff, Heim, Zilles, & Amunts, 2006). Percent signal change for the ROIs was extracted for each RS session as the mean signal over each ROI using the MarsBaR toolbox (version 0.44; Brett, Anton, Valabregue, & Poline, 2002). Subsequently, values were exported to SPSS 25 and entered into independent one-way ANOVAs with the factor "band" (LF, IM, HF). Significant effects of the "band" factor were followed up by Bonferroni-corrected post hoc tests. Time effects were not considered in this analysis as the factor "time" was not significant for absolute values of variability in cardiac and respiratory data.

3 | RESULTS

3.1 | Peripheral physiology

We investigated changes in physiological parameters of heart rate and respiration during RS fMRI prior to, compared to, post NF as well as the differential contribution of different frequency bands of ANS activity. For the heart rate (HR), average frequency decreased ($t(65) = 5.7$, $p < .001$) while RMSSD ($t(65) = -2.1$, $p = .04$) and LF power ($t(65) = -3.08$, $p < .01$) increased after NF. In the case of respiration, no changes were observed for average frequency and power in the three bands (all $p > .15$; Table 1).

The HRV power values were skewed (LF: 2.47 ± 0.21; IM: 2.65 ± 0.21; HF: 2.70 ± 0.21), and therefore, logarithmically transformed. A 2-by-3 rmANCOVA with the ln-transformed LF/IM/HF power data compared the effect of different frequency bands ("bands") on power in HRV, before and after NF ("repetition") with age as covariate and gender as between-subjects factor (see Table 2). Mauchly's Test of Sphericity indicated dependence for the factor "bands" ($\chi^2(2) = 10.8$, $p < .01$), and therefore, Greenhouse-Geisser correction was applied ($\varepsilon = 0.86$). The factor "repetition" did not yield significance ($F(1,63) = 0.32$, $p = .57$). However, the power differed significantly between the frequency bands ($F(1.72, 108.59) = 19.80$, $p < .001$). Bonferroni-corrected post hoc tests revealed significant differences in all pairwise comparisons between the bands (all $p < .022$). There was no significant interaction between repetition and bands ($F(2,126) = 1.60$, $p = .21$). The power in the different frequency bands was negatively associated with the age of the participants ($F(1,63) = 41.38$, $p < .001$), whereas the participants' gender did not have an effect ($F(1,63) = 0.001$, $p = .99$). A second 2-by-3 rmANCOVA was computed for variability in respiratory data (Table 2). The respiratory power values were skewed (LF: 1.19 ± 0.21; IM: 1.54 ± 0.21; HF: −0.22 ± 0.21), and therefore, transformed with a Box-Cox

TABLE 1 Absolute values of heart and respiration parameters during RS at Rest1 and Rest2

	Mean	Rest1	Rest2	Two-sided paired *t* test
HR [bpm]	66.5 (7.6)	68.0 (7.7)	65.0 (7.2)	**$t(65) = 5.70, p < .001$**
RMSSD/HRV [ms]	47.8 (31.2)	45.3 (28.3)	50.2 (34.0)	**$t(65) = -2.1, p = .04$**
Respiration [bpm]	4.01 (1.00)	3.96 (0.88)	4.06 (1.11)	$t(67) = -1.38, p = .17$
RMSSD/Resp [ms]	1.17 (0.35)	1.18 (0.37)	1.15 (0.33)	$t(65) = 0.82, p = .42$
HRV [ln (power)]				
LF	6.04 (0.83)	5.90 (0.76)	6.14 (0.88)	**$t(65) = -3.08, p < .01$**
IM	5.83 (1.09)	5.80 (1.04)	5.84 (1.15)	$t(65) = -0.55, p = .58$
HF	6.33 (1.30)	6.26 (1.34)	6.36 (1.28)	$t(65) = -1.22, p = .23$
Respiratory variability [Box-Cox-transform (power)]				
LF	1.28 (0.10)	1.09 (0.04)	1.10 (0.04)	$t(65) = -0.55, p = .59$
IM	1.25 (0.09)	1.09 (0.03)	1.09 (0.03)	$t(65) = 0.45, p = .65$
HF	1.38 (0.10)	1.14 (0.04)	1.14 (0.04)	$t(65) = 0.61, p = .55$

Bold values highlight significance of tests.

TABLE 2 Repeated-measures ANCOVA of power bands in HRV and respiratory variability

Parameter	Source	Partial η^2	*F*	*p*
HRV [ln (power)]	Repetition	0.005	0.32	.57
	Band	0.24	19.80	**<.001**
	Repetition × Band	0.03	1.60	.21
Respiratory variability [Box-Cox-transform (power)]	Repetition	0.003	0.19	.66
	Band	0.22	17.62	**<.001**
	Repetition × Band	0.006	0.35	.71

Bold values highlight significance of tests.

transformation ($\lambda = 0.05$). There was a significant difference between the three frequency bands ($F(2, 126) = 17.62$, $p < .001$), but power did not change from before to after NF ($F(1, 63) = 0.19$, $p = .66$). Bonferroni-corrected post hoc tests for frequency bands revealed significant differences in pair-wise comparisons of HF and LF bands, and HF and IM bands (all $p < .01$) and a trend-level effect between the IM and LF bands ($p = .09$). No interaction emerged ($F(2, 130) = 0.35$, $p = .71$), and gender ($F(1,63) = 2.51$, $p = .12$) and age ($F(1,63) = 2.89$, $p = .09$) suggested only trend-level effects.

Finally, to explore physiological significance of the different frequencies, Pearson correlation coefficients between the session-wise time courses of LF, IM, and HF bands of cardiac and respiratory data were calculated and revealed significant correlation coefficients between respiration and cardiac variability within the respective frequency band (Figure 2). For statistical confirmation, a 3-by-3 rmANOVA was computed. Mauchly's Test of Sphericity indicated dependence for all factors (all $p < .001$), and therefore, Greenhouse-Geisser correction (ε: HRV = 0.87, Resp = 0.76, HRV × Resp = 0.49) was applied. This analysis revealed a significant main effect for respiration ($F(1.51, 197.8) = 32.0$, $p < .001$) but not for cardiac data ($F(1.7, 228.3) = 2.5$, $p = .09$) as well as a significant interaction between cardiac and respiratory variability ($F(1.96, 256.7) = 44.7$, $p < .001$). The interaction suggests common functions of the distinct ANS bands across HR and respiration regulation. In particular, the IM band correlation had the strongest transmodal interaction as compared to the LF and HF bands.

3.2 | fMRI results

3.2.1 | Whole-brain GLM analysis

Different neural networks were involved in the regulation of the distinct physiological functions (see Appendix B—B.1 to B.5 for LF and HF results). Activations of the pre and postcentral gyri were associated with IM band activity in HRV. In addition, the HRV IM band recruited areas such as precuneus, PCC, MCC, and the middle/posterior insula extending into secondary somatosensory cortex (SS2; see Figure 3 and Table 3). In the respiratory system, IM fluctuations yielded overlap with HRV IM band activations in the middle/posterior insula, SS2 (see Figure 4b), and primary sensory cortex (see Table 4).

3.2.2 | ROI analysis

The ROI analysis investigated whether the mean percent signal change of the eight ROIs differed between the LF, IM, and HF band (see Figure 5). All one-way ANOVAs of the ROIs for variability in respiratory data yielded significant main effects while only the amygdala, parietal and sensorimotor ROI were significant for HRV. Analogously to the whole-brain analysis, the LF band was related to deactivations in the ACC, amygdala, parietal and sensorimotor ROIs for cardiac data and all ROIs for respiratory data. Bonferroni corrected post hoc tests for HRV showed an increased activation in the amygdala and parietal and sensorimotor ROIs in the IM compared to the LF band whereas the difference between LF and HF was only significant for the parietal and sensorimotor ROI. In line with the whole-brain analysis, activation clusters in respiratory data were most extended in the HF band. The difference between HF and LF was significant for ACC, MCC, PCC, amygdala, PAG, parietal, and insula ROIs, whereas, the HF band was only significantly different from the IM band in the ACC and PAG. For the IM band in respiratory data, activation was higher than the LF band in amygdala, parietal and insula ROIs. However, for these contrasts the difference between LF and HF was only not significant in the sensorimotor ROI. In combination with the heightened cardiac IM band activation, this suggests a specific involvement of this area for the IM band. Comparing the

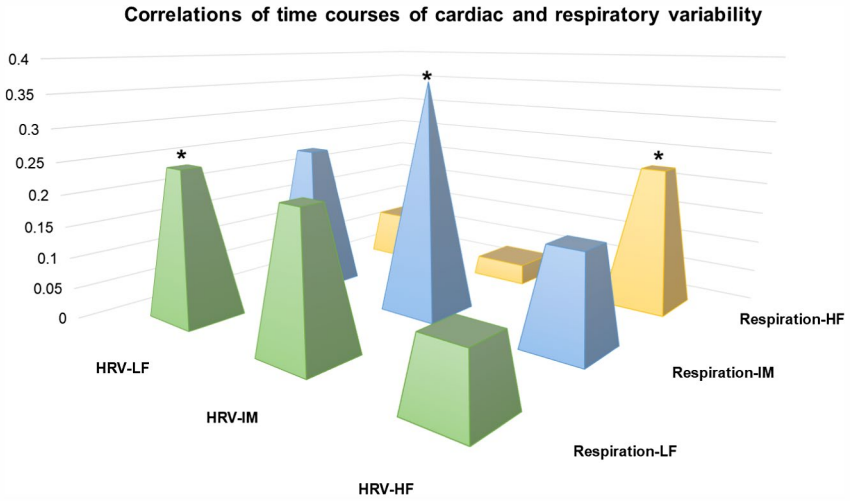

FIGURE 2 Correlation coefficients between cardiac and respiratory power in the three frequency bands (LF, IM, and HF) across the group. The correlations were highest within each specific band, suggesting a common physiological mechanism of the ANS modulation with separate output modality for each band. In particular, coupling between HRV and respiration was highest in the IM band

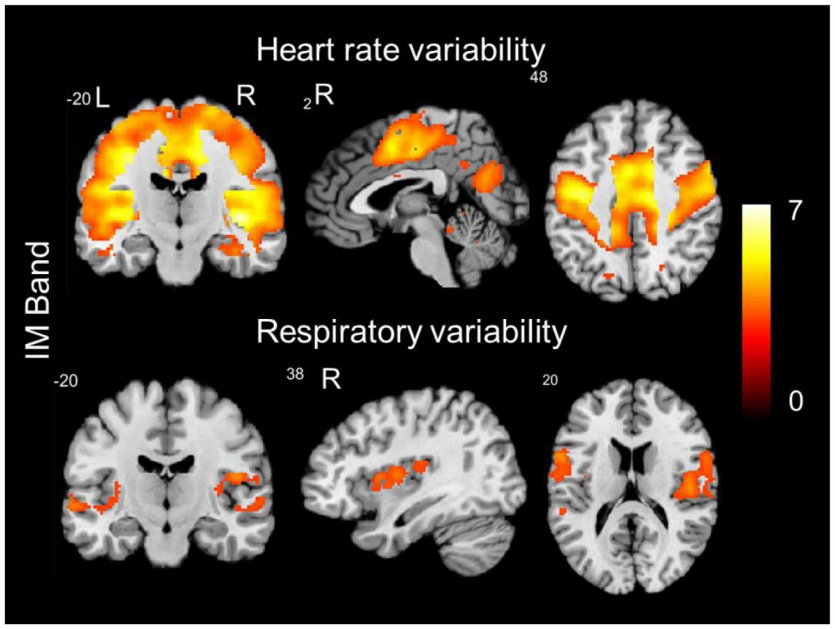

FIGURE 3 Neural correlates of variability in the cardiac and the respiratory data for the IM band (0.12–0.18 Hz). Upper panel: HRV in the IM band was positively related to activation in midline structures (MCC, PCC, precuneus) as well as mid and posterior insula and pre and postcentral gyri. Lower panel: The correlation patterns in the respiratory IM band were overlapping but less pronounced compared to HRV and were selectively found in bilateral mid and posterior insula as well as rolandic operculum (SS2) and precentral gyri. All maps are corrected at FWE-cluster level $p < .05$ (after voxel level threshold $p < .001$)

TABLE 3 BOLD correlates of heart rate variability for the IM band components

HRV-IM (positive)	MNI coordinates [mm]				
Location	*x*	*y*	*z*	Volume [voxel]	Peak *t*-value
Insula_R	40	−18	4	46,910	6.578
Postcentral_L	−52	−8	18	46,910	6.120
Temporal_Sup_L	−44	−34	18	46,910	5.971
Precentral_L	−34	−20	46	46,910	5.922
Rolandic_Oper_R	48	−24	22	46,910	5.920
Temporal_Sup_R	60	−4	4	46,910	5.869
Postcentral_L	−18	−30	62	46,910	5.864
Insula_L	−32	−16	20	46,910	5.858

Note: Clusters reported at $p < .05$ FWE-corrected ($p < .001$ voxelwise threshold).

ROI findings between cardiac and respiratory data, cardiac IM band and respiratory HF band yielded similar activation patterns in midline, subcortical, and brainstem areas.

4 | DISCUSSION

Using resting-state functional magnetic resonance imaging (RS fMRI), we investigated neural correlates of ANS activity as reflected in cardiac and respiratory control. We focused on intermediate (IM) band variability in cardiac and respiratory rates in addition to the well-established low frequency (LF) and high frequency bands (HF). In 41 healthy volunteers, the analysis segregated networks reflecting the regulation of the IM as well as the LF and HF bands. The IM band in respiratory and cardiac variability shared insular and sensorimotor cortex involvement suggesting interoceptive mechanisms. Frequency band-specific activations emerged in midline and limbic ROIs in particular associated with higher global HF, cardiac IM, and lower respiratory LF oscillations. These findings are in line with previous findings on the relation of HRV and RS fMRI (e.g., Thayer, Åhs, Fredrikson, Sollers, & Wager, 2012). The detailed analysis of different frequency components and modalities of ANS regulation may provide further insight in physiological self-regulation during rest.

4.1 | Frequency bands

The negative correlation of the LF band with the BOLD response was supported by an exploratory ROI analysis, which revealed widespread deactivations in the LF band (cf. Critchley, Melmed, Featherstone, Mathias, & Dolan, 2002). Furthermore, HF-HRV was associated with activations in core ANS regulation areas encompassing the insula, MCC, and supramarginal/angular gyrus (Beissner et al., 2013). Both findings are in line with the literature and are discussed in more detail in Appendix C.

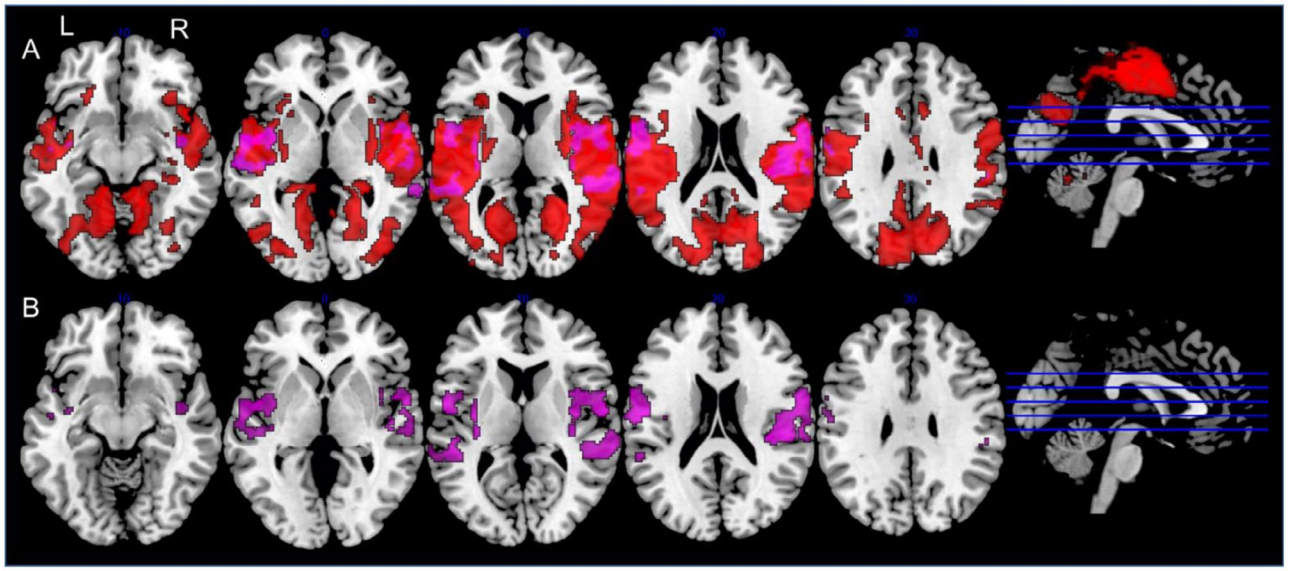

FIGURE 4 Conjunction analyses. (a) Conjunction map of cardiac IM band (red) and respiratory IM band (blue). Maps depict an overlap (purple) in mid/posterior insula and SS2. (b) Conjunction analysis of IM band in cardiac and respiratory data, suggesting a convergent role of interoceptive perception areas for IM band activation. All maps are corrected at FWE-cluster level $p < .05$ (after voxel level threshold $p < .001$)

TABLE 4 BOLD correlates of respiratory variability for the IM band components

Resp-IM (positive)	MNI coordinates [mm]				
Location	*x*	*y*	*z*	Volume [voxel]	Peak *t*-value
Precentral_L	−60	6	22	1,759	4.225
Temporal_Sup_L	−58	−4	−2	1,759	4.096
Temporal_Sup_L	−48	−40	10	1,759	3.975
Insula_L	−36	−2	0	1,759	3.931
Rolandic_Oper_R	48	−20	20	2,087	3.989
Rolandic_Oper_R	52	−6	14	2,087	3.887
Rolandic_Oper_R	46	−12	18	2,087	3.870
Temporal_Sup_R	64	−30	10	2,087	3.840

Note: Clusters reported at $p < .05$ FWE-corrected ($p < .001$ voxelwise threshold).

The IM band has been implicated in the regulation of arousal. In particular, during AT, participants displayed a higher coupling in the IM band, between the physiological subsystems (Perlitz, Lambertz, et al., 2004). The present study replicated IM band fluctuations in the PPG signal recorded from the left index finger as well as in the respiratory signal during RS fMRI. The correlations between the cardiac and the respiratory power fluctuations were highest within specific frequency bands. This indicates a common mechanism of ANS regulation segregated between the frequency bands or, in other words, that the generators acted across modalities affecting respiration as well as heart rate. Interestingly, the correlation within the IM band was higher than within LF and HF bands. Such synchronized mechanisms in the IM band power in cardiac and respiratory data, may point at a shared CNS pathway for the two modalities reflected by their common BOLD activation in the mid and posterior insula and SS2. Furthermore, the precentral gyrus activity may support recent findings of synchronous time courses in the left brainstem and left precentral gyrus during IM band activity (Pfurtscheller et al., 2019). The data support a growing body of evidence indicating that, in addition to the commonly considered LF and HF bands, the IM band represents a relevant physiological component. In particular, the IM band during RS fMRI was associated with activity in structures subserving interoception.

4.2 | Cerebral correlates of ANS regulation

In the present ROI analysis, IM band contributions were more prominent in cardiac compared to respiratory data.

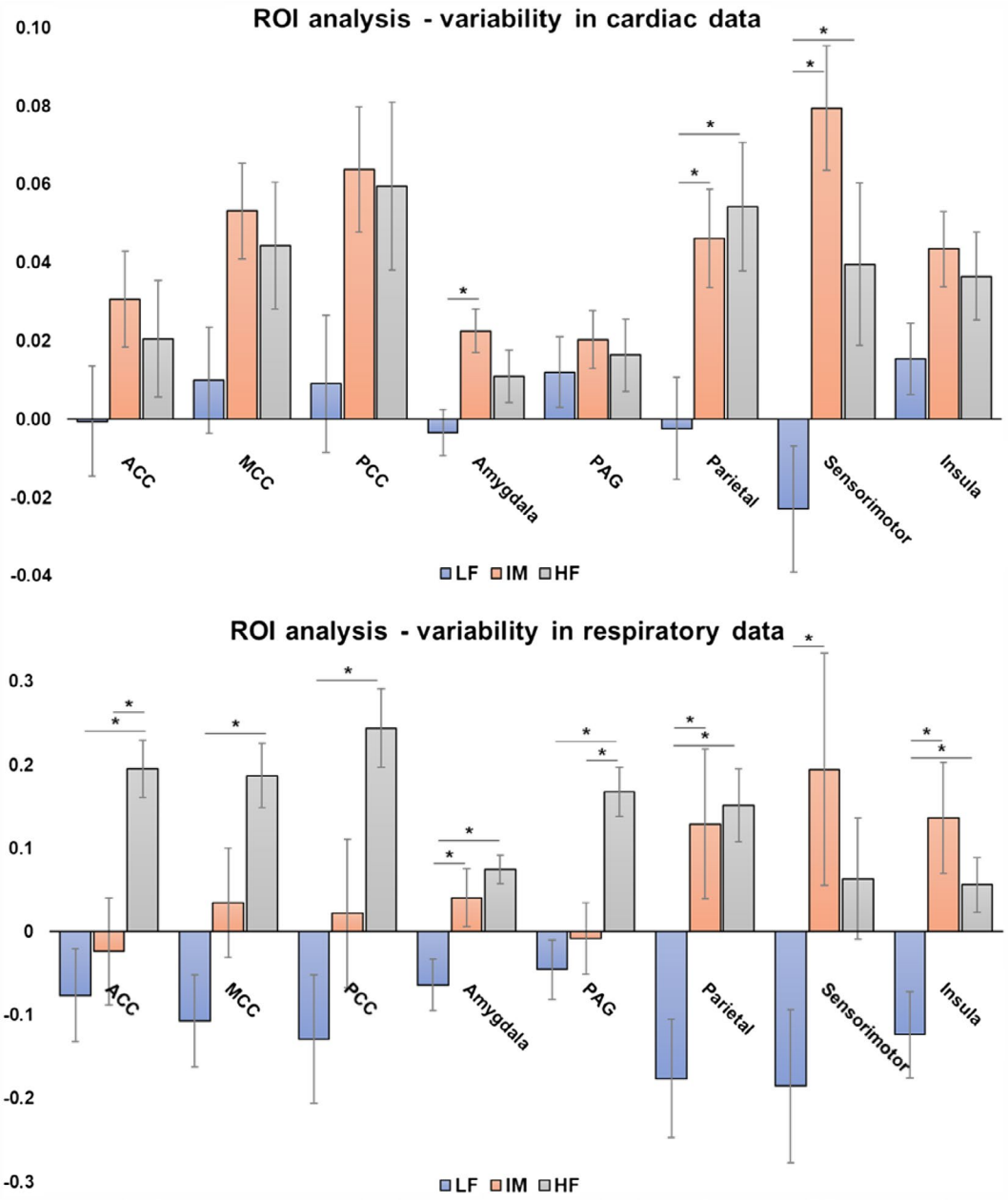

FIGURE 5 Region of interest (ROI) analysis for (a) cardiac and (b) respiratory variability. Independent univariate ANOVAs with factor band were computed for each ROI. (a) In cardiac data, Bonferroni corrected post hoc tests indicate that the IM band is associated with larger activation compared to the LF band in the amygdala, the parietal and sensorimotor ROIs with a general trend toward higher activation within the IM band, supporting the widespread activation pattern in the whole brain map. (b) Bonferroni corrected post hoc tests showed significantly increased activation in the HF band compared to LF and IM band for ACC and PAG as well as the MCC, PCC, parietal areas and insula compared to only LF band. IM band activation was significantly different from the LF band in amygdala, parietal and sensorimotor areas as well as the insula. A non-significant difference in the sensorimotor areas between the LF and HF bands, combined with the high activation in the HRV data, indicate a converging role of sensorimotor areas for the IM band. Abbreviations: ACC: anterior cingulate cortex; MCC: middle cingulate cortex; PCC: posterior cingulate cortex; PAG: periaqueductal grey; Parietal: composite of bilateral parietal areas; Sensorimotor: composite of sensory and motor areas. Error bars indicate confidence interval

Similarly, the cardiac IM band activity was associated with widespread activation in areas related to autonomic regulation as well as the default mode network (DMN), whereas, the respiratory IM influence was restricted to the mid/posterior insula and the SS2. Consequently, cardiac and respiratory activations overlapped in the mid/posterior insula and the SS2. These regions have been considered the primary interoceptive cortex, analogous to the primary visual or auditory cortex. Its function encompasses the sensorimotor processing of somato- and viscerosensory stimuli (e.g., Kurth et al., 2010) reflecting central mechanisms of ANS regulation.

The association of the IM band activity with interoceptive perception is also in line with studies indicating its relation to states of relaxation (Perlitz, Cotuk, Schiepek, et al., 2004). In particular, the insula seems to play a key role here. According to Craig (2002), the sensory system can be divided into interoceptive/nociceptive and exteroceptive/proprioceptive components. In this model, the insula integrates information from both modalities, as it receives interoceptive sensory information from ascending sensory pathways as well as exteroceptive information (visual/auditory) (Craig & Craig, 2009). The neural correlates of interoception reflecting the lowest level of processing were observed in the posterior insula. In particular, dorsal posterior insula activation is consistently found in studies investigating the experience of painful stimuli, which is part of the interoceptive network (Craig, 2002). Blefari and colleagues (2017) found that activation in the bilateral rolandic operculum (a region closely interconnected to posterior insula) was related to the integration of interoceptive-exteroceptive bodily signals. Furthermore, lesions of this region have been shown to disrupt interoceptive perception (e.g., Greenspan & Winfield, 1992). Interestingly, previous studies have shown that the IM band power can be disrupted by painful cold stimuli (Krautstrunk & Schmid-Schönbein, 2008; Lampmann & Petzold, 2006), a process sharing a common pathway with visceral (and other) interoceptive processing. The insula, as a core autonomic regulation area, was not only activated in the IM, but also in the HF band of both, cardiac and respiratory data. However, the cardiac HF band revealed more right anterior insula activation. Anterior parts of the insula have been related to conscious awareness and subjective evaluation of interoceptive signals (Craig, 2002; Craig & Craig, 2009; Critchley, Wiens, Rotshtein, Öhman, & Dolan, 2004). Furthermore, the reduced HRV and higher risk of sudden death in patients with stroke in the middle cerebral artery, indicate the importance of the (especially right) anterior insula for autonomic control (e.g., Tokgözoglu et al., 1999). Based on our findings and previous evidence, we suggest that the IM band power may be related to a shared pathway of interoceptive and nociceptive stimuli. These stimuli may be related to recruitment of sensory perception areas within the mid and posterior insula and SS2 rather than the conscious processing of internal and external sensory and visceral information. We think that our data warrant this interpretation linking the IM band and interoceptive processing. However, as no measures of interoceptive processes could be collected during RS fMRI, interpretations about interoception remain speculative.

Neural correlates of the cardiac IM power compared to the respiratory IM power showed a more widespread pattern of activation extending into the DMN areas. Considering that interoception is one of the main drivers of RS brain activity (e.g., Wong, Massé, Kimmerly, Menon, & Shoemaker, 2007), it is not surprising that the IM band correlates with BOLD signal changes in these areas.

Jerath and Crawford (2015) argued the importance of cardiorespiratory oscillations and the DMN in building a foundation on which other neural activity and consciousness can arise. The DMN is comprised of hubs such as the PCC and precuneus and has been linked to internally oriented cognitive states (Buckner, Andrews-Hanna, & Schacter, 2008). With respect to DMN areas, it is remarkable how similar the patterns of the cardiac IM and respiratory HF band are in the ROI analysis. Furthermore, both whole-brain maps show overlap in the precuneus/PCC, (left) intra parietal lobe and the ACC, areas that have also been associated with parasympathetic modulatory functions (Beissner et al., 2013). This overlap of HRV IM and respiration HF bands in core DMN areas may by suggestive of a resting mental state, rather than physiological oscillations at certain bands. A possible link between neural mechanisms of the cardiac IM band and the respiratory HF band should be further investigated.

4.3 | Clinical outlook and limitations

Over the past decade, the study of HRV has received much attention as it can tell us about the body's capability to adaptively modulate the ANS, an essential function for our physiological and psychological well-being (Thayer, Åhs, Fredrikson, Sollers, & Wager, 2012). Meta-analyses have shown the predictive value of HF-HRV for psychological well-being, for example, low resting HF-HRV has been linked to psychiatric disorders such as depression (e.g., Kemp et al., 2010) and schizophrenia (Montaquila, Trachik, & Bedwell, 2015) which may be related to its role in self-regulatory top-down control capacity (Holzman & Bridgett, 2017). Further, a better understanding of the coupling between brain activation and peripheral physiological regulation may enable a better reduction of artefacts in the widely applied RS fMRI (Tong, Hocke, & Frederick, 2019; Zweerings et al., 2019) and thereby adding to its clinical and scientific value.

We assessed the effect of a neurofeedback protocol on the ANS measures. Mean HR decreased significantly from pre to post measurement whereas RMSSD of the cardiac data increased. The decrease of the HR may be related to a general decrease of arousal over time (Weber, Behr, Tamborini, Ritterfeld, & Mathiak, 2009). Similarly, the increase in RMSSD may be related to a reduced stress within the scanner environment over time. Both changes, however, did not significantly affect ANS regulation in either of the bands or the underlying neural networks.

In the present study, we have investigated the IM frequency band in cardiac and respiratory data. The IM band has been linked to AT, an emotion-focused coping strategy that has been deemed beneficial for mental health (e.g., Lim & Kim, 2014) by shifting ANS functioning toward parasympathetic and away from sympathetic regulation (Mitani,

Fujita, Sakamoto, & Shirakawa, 2006; Miu, Heilman, & Miclea, 2009). Similarly, such a shift in ANS functioning has been shown to follow osteopathic manipulative treatment (OMT; Ruffini et al., 2015). However, there is a debate about the specific neurobiological mechanisms of AT and OMT. In the present study, IM band fluctuations in cardiac and respiratory data correlated with BOLD signal responses in interoceptive perceptions areas, namely, the posterior insula and SS2, suggesting that IM band power could be used as a marker for interoceptive processes. Interestingly, altered interoceptive states are also part of many psychiatric disorders such as schizophrenia (Ardizzi et al., 2016; Linnman, Coombs, Goff, & Holt, 2013) and depression (Avery et al., 2014; Paulus & Stein, 2010; Wiebking et al., 2015), suggesting that interoception has a broad range of clinical implications. Accordingly, it may be worthwhile to further investigate a possible link between interoceptive processes and IM band power in patient populations with disturbed interoceptive processing.

This study was the first to investigate the neural underpinnings of the IM band in humans during RS fMRI, and thus, contains some limiting factors due to its explorative nature and lack of replication. First, due to the technical circumstance of fMRI measurements, the methodology of investigating the IM band was restricted to PPG recorded from the finger. PPG waveform is significantly affected by the measurement site (e.g., Hartmann et al., 2019), which raises the question whether there are differences in IM band depending on PPG sensor location. Studies applying different pulse measures have found, for example, that whereas rhythmical oscillations in laser Doppler flow were around 0.13 Hz in the forehead during nonpulsatile cardiopulmonary bypass, oscillations at the finger were around 0.07 Hz (harmonic of the IM band) (Podgoreanu et al., 2002). However, IM band activity was higher in both finger and forehead PPG as well as ECG-derived HRV during relaxation (Perlitz, Cotuk, Lambertz, et al., 2004). Considering the high correlation between PPG- and ECG-derived HRV indices (Schäfer & Vagedes, 2013), similar findings relating to the IM band from these different methods are not surprising. However, further investigations of the IM band at different measurement sites in relation to its mechanism and differences between PPG and ECG in IM and other frequency bands are needed. Second, there has been some controversy around the significance of the IM band and some authors have questioned its predictive value as, in some people, it was prevalent irrespective of their cognitive state (Mück-Weymann, 2000). Third, the interaction between cardiac and respiratory data was only investigated on the peripheral physiological level. It would be important to test whether a similar activation in interoceptive perception areas would be observed during phases of increased correlation or coherence. Finally, during RS fMRI measurements, we had no record of participants' thoughts. Therefore, hypotheses about ongoing interoceptive processing remain speculative so far.

4.4 | Conclusion

We demonstrated dissociable neural networks underlying cardiac and respiratory variability in the IM band during RS fMRI. The IM band in both peripheral physiological modalities was related to overlapping activations in the insula and somatosensory cortices, indicating a functional association with interoception. Future fMRI studies should investigate the emergence of the IM band in clinical populations or groups that have been trained on interoceptive processes. Considering previous studies, practitioners of meditation or AT could be studied to investigate the effect of such specific self-regulation technique on the distinct recruitment of interoceptive perception areas. The association of the IM band with AT and its neural correlates may address the question of the mechanism behind such body-focused relaxation technique and may potentially bridge the gap between its psychological and physiological effects.

ACKNOWLEDGMENTS

We thank Sarah Bleich, Arndt Brandl and Manouela Kosmadaki for their assistance with participant recruitment and data collection as well as the Brain Imaging Facility, a Facility of the Interdisciplinary Center for Clinical Research (IZKF) Aachen within the Faculty of Medicine at RWTH Aachen University for their technical support.

CONFLICT OF INTEREST

The authors declare that there is no conflict of interest regarding the publication of this article.

ORCID

Micha Keller https://orcid.org/0000-0002-5221-4890
Jana Zweerings https://orcid.org/0000-0002-5724-1054
Halim Ibrahim Baqapuri https://orcid.org/0000-0003-4360-3621
Klaus Mathiak https://orcid.org/0000-0002-2276-7726

REFERENCES

Agcaoglu, O., Wilson, T. W., Wang, Y. P., Stephen, J., & Calhoun, V. D. (2019). Resting state connectivity differences in eyes open versus eyes closed conditions. *Human Brain Mapping*, *40*(8), 2488–2498. https://doi.org/10.1002/hbm.24539

Ardizzi, M., Ambrosecchia, M., Buratta, L., Ferri, F., Peciccia, M., Donnari, S., … Gallese, V. (2016). Interoception and positive symptoms in schizophrenia. *Frontiers in Human Neuroscience*, *10*, 379. https://doi.org/10.3389/fnhum.2016.00379

Avery, J. A., Drevets, W. C., Moseman, S. E., Bodurka, J., Barcalow, J. C., & Simmons, W. K. (2014). Major depressive disorder is associated with abnormal interoceptive activity and functional connectivity in the insula. *Biological Psychiatry*, *76*(3), 258–266. https://doi.org/10.1016/j.biopsych.2013.11.027

Beissner, F., Meissner, K., Bär, K.-J., & Napadow, V. (2013). The autonomic brain: An activation likelihood estimation meta-analysis for

central processing of autonomic function. *Journal of Neuroscience*, *33*(25), 10503–10511. https://doi.org/10.1523/JNEUROSCI.1103-13.2013

Birn, R. M. (2012). The role of physiological noise in resting-state functional connectivity. *NeuroImage*, *62*(2), 864–870. https://doi.org/10.1016/j.neuroimage.2012.01.016

Blefari, M. L., Martuzzi, R., Salomon, R., Bello-Ruiz, J., Herbelin, B., Serino, A., & Blanke, O. (2017). Bilateral Rolandic operculum processing underlying heartbeat awareness reflects changes in bodily self-consciousness. *European Journal of Neuroscience*, *45*(10), 1300–1312. https://doi.org/10.1111/ejn.13567

Brett, M., Anton, J.-L., Valabregue, R., & Poline, J.-B. (2002). Region of interest analysis using an SPM toolbox. *Paper presented at the 8th international conference on functional mapping of the human brain*. Sendai, Japan.

Buckner, R. L., Andrews-Hanna, J. R., & Schacter, D. L. (2008). The brain's default network. *Annals of the New York Academy of Sciences*, *1124*(1), 1–38. https://doi.org/10.1196/annals.1440.011

Camm, A. J., Malik, M., Bigger, J. T., Breithardt, G., Cerutti, S., Cohen, R. J., … Kleiger, R. (1996). Heart rate variability: Standards of measurement, physiological interpretation and clinical use. Task force of the European Society of Cardiology and the North American Society of pacing and electrophysiology. *Circulation*, *93*, 1043–1065.

Craig, A. D. (2002). How do you feel? Interoception: The sense of the physiological condition of the body. *Nature Reviews Neuroscience*, *3*(8), 655–666. https://doi.org/10.1038/nrn894

Craig, A. D., & Craig, A. (2009). How do you feel–now? The anterior insula and human awareness. *Nature Reviews Neuroscience*, *10*(1), 59–70. https://doi.org/10.1038/nrn2555

Critchley, H. D., Melmed, R. N., Featherstone, E., Mathias, C. J., & Dolan, R. J. (2002). Volitional control of autonomic arousal: A functional magnetic resonance study. *NeuroImage*, *16*(4), 909–919. https://doi.org/10.1006/nimg.2002.1147

Critchley, H. D., Wiens, S., Rotshtein, P., Öhman, A., & Dolan, R. J. (2004). Neural systems supporting interoceptive awareness. *Nature Neuroscience*, *7*(2), 189–195. https://doi.org/10.1038/nn1176

Eickhoff, S. B., Heim, S., Zilles, K., & Amunts, K. (2006). Testing anatomically specified hypotheses in functional imaging using cytoarchitectonic maps. *NeuroImage*, *32*(2), 570–582. https://doi.org/10.1016/j.neuroimage.2006.04.204

Ernst, J.-P., & Petzold, E. R. (2012). *Dynamik des 0, 15-Hz-Rhythmusbandes in der Hautdurchblutung bei Musikexposition* (Doctoral dissertation). Hochschulbibliothek der Rheinisch-Westfälischen. Technischen Hochschule Aachen.

Evans, K. C. (2010). Cortico-limbic circuitry and the airways: Insights from functional neuroimaging of respiratory afferents and efferents. *Biological Psychology*, *84*(1), 13–25. https://doi.org/10.1016/j.biopsycho.2010.02.005

Gaser, C., & Dahnke, R. (2016). CAT—A computational anatomy toolbox for the analysis of structural MRI data. *HBM*, *2016*, 336–348.

Glover, G. H., Li, T. Q., & Ress, D. (2000). Image-based method for retrospective correction of physiological motion effects in fMRI: RETROICOR. *Magnetic Resonance in Medicine*, *44*(1), 162–167. https://doi.org/10.1002/1522-2594(200007)44:1<162:aid-mrm23>3.0.co;2-e

Greenspan, J. D., & Winfield, J. A. (1992). Reversible pain and tactile deficits associated with a cerebral tumor compressing the posterior insula and parietal operculum. *Pain*, *50*(1), 29–39. https://doi.org/10.1016/0304-3959(92)90109-o

Hartmann, V., Liu, H., Chen, F., Qiu, Q., Hughes, S., & Zheng, D. (2019). Quantitative comparison of photoplethysmographic waveform characteristics: Effect of measurement site. *Frontiers in Physiology*, *10*, 198. https://doi.org/10.3389/fphys.2019.00198

Hidalgo-Muñoz, A. R., Béquet, A. J., Astier-Juvenon, M., Pépin, G., Fort, A., Jallais, C., … Gabaude, C. (2018). Respiration and heart rate modulation due to competing cognitive tasks while driving. *Frontiers in Human Neuroscience*, *12*, 525. https://doi.org/10.3389/fnhum.2018.00525

Holzman, J. B., & Bridgett, D. (2017). Heart rate variability indices as bio-markers of top-down self-regulatory mechanisms: A meta-analytic review. *Neuroscience Biobehavioral Reviews*, *74*, 233–255. https://doi.org/10.1016/j.neubiorev.2016.12.032

Jerath, R., & Crawford, M. W. (2015). Layers of human brain activity: A functional model based on the default mode network and slow oscillations. *Frontiers in Human Neuroscience*, *9*, 248. https://doi.org/10.3389/fnhum.2015.00248

Kasper, L., Bollmann, S., Diaconescu, A. O., Hutton, C., Heinzle, J., Iglesias, S., … Stephan, K. E. (2017). The PhysIO toolbox for modeling physiological noise in fMRI data. *Journal of Neuroscience Methods*, *276*, 56–72. https://doi.org/10.1016/j.jneumeth.2016.10.019

Kemp, A. H., Quintana, D. S., Gray, M. A., Felmingham, K. L., Brown, K., & Gatt, J. M. (2010). Impact of depression and antidepressant treatment on heart rate variability: A review and meta-analysis. *Biological Psychiatry*, *67*(11), 1067–1074. https://doi.org/10.1016/j.biopsych.2009.12.012

Kettunen, J., & Keltikangas-Järvinen, L. (2001). Intraindividual analysis of instantaneous heart rate variability. *Psychophysiology*, *38*(4), 659–668. https://doi.org/10.1111/1469-8986.3840659

Krautstrunk, H. G., & Schmid-Schönbein, H. (2008). *Objektivierende Registrierung holistischer, neurophysiologischer Sprünge beim selbstaffizierten Schmerzereignis im sogenannten cold pressure test* (No. RWTH-CONV-112790). Aachen: Lehr-und Forschungsgebiet Physiologie.

Kurth, F., Zilles, K., Fox, P. T., Laird, A. R., & Eickhoff, S. B. (2010). A link between the systems: Functional differentiation and integration within the human insula revealed by meta-analysis. *Brain Structure Function*, *214*(5–6), 519–534. https://doi.org/10.1007/s00429-010-0255-z

Lambertz, M., & Langhorst, P. J. (1998). Simultaneous changes of rhythmic organization in brainstem neurons, respiration, cardiovascular system and EEG between 0.05 Hz and 0.5 Hz. *Journal of the Autonomic Nervous System*, *68*(1–2), 58–77. https://doi.org/10.1016/S0165-1838(97)00126-4

Lambertz, M., Vandenhouten, R., Grebe, R., & Langhorst, P. (2000). Phase transitions in the common brainstem and related systems investigated by nonstationary time series analysis. *Journal of the Autonomic Nervous System*, *78*(2–3), 141–157. https://doi.org/10.1016/S0165-1838(99)00072-7

Lampmann, M., & Petzold, E. R. (2006). *Kryodentalstimulation zur Objektivierung kältereizinduzierter, psychovegetativer Reaktionen* (No. RWTH-CONV-123489). Aachen: Medizinische Fakultät.

Langhorst, P., Lambertz, M., & Schulz, G. (1986).Assessment of rhythmicity in the visceral nervous system. In B. Lown, A. Malliani, & M. Prosdocimi (Eds.), *Neural mechanisms and cardivascular disease* (pp. 133–144). Padova, Italy: Liviana. (Fidia research series 5).

Lim, S.-J., & Kim, C. (2014). Effects of autogenic training on stress response and heart rate variability in nursing students. *Asian Nursing Research*, *8*(4), 286–292. https://doi.org/10.1016/j.anr.2014.06.003

Linnman, C., Coombs, G., III, Goff, D. C., & Holt, D. J. (2013). Lack of insula reactivity to aversive stimuli in schizophrenia. *Schizophrenia Research*, *143*(1), 150–157. https://doi.org/10.1016/j.schres.2012.10.038

Maldjian, J. A., Laurienti, P. J., Kraft, R. A., & Burdette, J. H. (2003). An automated method for neuroanatomic and cytoarchitectonic atlas-based interrogation of fMRI data sets. *NeuroImage*, *19*(3), 1233–1239. https://doi.org/10.1016/s1053-8119(03)00169-1

Mitani, S., Fujita, M., Sakamoto, S., & Shirakawa, T. (2006). Effect of autogenic training on cardiac autonomic nervous activity in high-risk fire service workers for posttraumatic stress disorder. *Journal of Psychosomatic Research*, *60*(5), 439–444. https://doi.org/10.1016/j.jpsychores.2005.09.005

Miu, A. C., Heilman, R. M., & Miclea, M. (2009). Reduced heart rate variability and vagal tone in anxiety: Trait versus state, and the effects of autogenic training. *Autonomic Neuroscience*, *145*(1–2), 99–103. https://doi.org/10.1016/j.autneu.2008.11.010

Montaquila, J. M., Trachik, B. J., & Bedwell, J. S. (2015). Heart rate variability and vagal tone in schizophrenia: A review. *Journal of Psychiatric Research*, *69*, 57–66. https://doi.org/10.1016/j.jpsychires.2015.07.025

Mück-Weymann, M. (2000). *Autonome Funktionskreise in Psychosomatik und Psychiatrie: Nicht-invasives Biomonitoring in der Psychopharmakotherapie*. Lage, Germany: Jacobs.

Paulus, M. P., & Stein, M. B. (2010). Interoception in anxiety and depression. *Brain Structure Function*, *214*(5–6), 451–463. https://doi.org/10.1007/s00429-010-0258-9

Perlitz, V., Cotuk, B., Lambertz, M., Grebe, R., Schiepek, G., Petzold, E. R., … Flatten, G. (2004). Coordination dynamics of circulatory and respiratory rhythms during psychomotor drive reduction. *Autonomic Neuroscience*, *115*(1–2), 82–93. https://doi.org/10.1016/j.autneu.2004.07.007

Perlitz, V., Cotuk, B., Schiepek, G., Sen, A., Haberstock, S., Schmid-Schönbein, H., … Flatten, G. (2004). Synergetik der hypnoiden Relaxation. *PPmP-Psychotherapie Psychosomatik Medizinische Psychologie*, *54*(06), 250–258. https://doi.org/10.1055/s-2003-814877

Perlitz, V., Lambertz, M., Cotuk, B., Grebe, R., Vandenhouten, R., Flatten, G., … Langhorst, P. (2004). Cardiovascular rhythms in the 0.15-Hz band: Common origin of identical phenomena in man and dog in the reticular formation of the brain stem? *Pflügers Archiv—European Journal of Physiology*, *448*(6), 579–591. https://doi.org/10.1007/s00424-004-1291-4

Pfurtscheller, G., Rassler, B., Schwerdtfeger, A. R., Klimesch, W., Andrade, A., Schwarz, G., & Thayer, J. F. (2019). "Switch-off" of respiratory sinus arrhythmia (RSA) may be associated with the activation of an oscillatory source (pacemaker) in the brain stem. *Frontiers in Physiology*, *10*, 939. https://doi.org/10.3389/fphys.2019.00939

Podgoreanu, M. V., Stout, R. G., El-Moalem, H. E., & Silverman, D. G. (2002). Synchronous rhythmical vasomotion in the human cutaneous microvasculature during nonpulsatile cardiopulmonary bypass. *Anesthesiology: The Journal of the American Society of Anesthesiologists*, *97*(5), 1110–1117. https://doi.org/10.1097/00000542-200211000-00012

Reyes del Paso, G. A., Langewitz, W., Mulder, L. J., Van Roon, A., & Duschek, S. (2013). The utility of low frequency heart rate variability as an index of sympathetic cardiac tone: A review with emphasis on a reanalysis of previous studies. *Psychophysiology*, *50*(5), 477–487. https://doi.org/10.1111/psyp.12027

Ritz, T., & Dahme, B. (2006). Implementation and interpretation of respiratory sinus arrhythmia measures in psychosomatic medicine: Practice against better evidence? *Psychosomatic Medicine*, *68*(4), 617–627. https://doi.org/10.1097/01.psy.0000228010.96408.ed

Ruffini, N., D'Alessandro, G., Mariani, N., Pollastrelli, A., Cardinali, L., & Cerritelli, F. (2015). Variations of high frequency parameter of heart rate variability following osteopathic manipulative treatment in healthy subjects compared to control group and sham therapy: Randomized controlled trial. *Frontiers in Neuroscience*, *9*, 272. https://doi.org/10.3389/fnins.2015.00272

Schäfer, A., & Vagedes, J. (2013). How accurate is pulse rate variability as an estimate of heart rate variability? A review on studies comparing photoplethysmographic technology with an electrocardiogram. *International Journal of Cardiology*, *166*(1), 15–29. https://doi.org/10.1016/j.ijcard.2012.03.119

Schlamann, M., Naglatzki, R., de Greiff, A., Forsting, M., & Gizewski, E. R. (2010). Autogenic training alters cerebral activation patterns in fMRI. *International Journal of Clinical Experimental Hypnosis*, *58*(4), 444–456. https://doi.org/10.1080/00207144.2010.499347

Scholkmann, F., & Wolf, U. (2019). The pulse-respiration quotient: A powerful but untapped parameter for modern studies about human physiology and pathophysiology. *Frontiers in Physiology*, *10*, 371. https://doi.org/10.3389/fphys.2019.00371

Schwerdtfeger, A. R., Schwarz, G., Pfurtscheller, K., Thayer, J. F., Jarczok, M. N., & Pfurtscheller, G. (2019). Heart Rate Variability (HRV): From brain death to resonance breathing at 6 breaths/minute. *Clinical Neurophysiology*, *131*(3), 676–693. https://doi.org/10.1016/j.clinph.2019.11.013

Selvaraj, N., Jaryal, A., Santhosh, J., Deepak, K. K., & Anand, S. (2008). Assessment of heart rate variability derived from finger-tip photoplethysmography as compared to electrocardiography. *Journal of Medical Engineering Technology*, *32*(6), 479–484. https://doi.org/10.1080/03091900701781317

Shaffer, F., & Ginsberg, J. (2017). An overview of heart rate variability metrics and norms. *Frontiers in Public Health*, *5*, 258. https://doi.org/10.3389/fpubh.2017.00258

Silverman, D. G., & Stout, R. G. (2002). Distinction between atropine-sensitive control of microvascular and cardiac oscillatory activity. *Microvascular Research*, *63*(2), 196–208. https://doi.org/10.1006/mvre.2001.2385

Silverman, D. G., Stout, R. G., Lee, F. A., & Ferneini, E. M. (2001). Detection and characterization of cholinergic oscillatory control in the forehead microvasculature in response to systemic α-agonist infusion in healthy volunteers. *Microvascular Research*, *61*(1), 144–147. https://doi.org/10.1006/mvre.2000.2283

Smith, S. M., Beckmann, C. F., Andersson, J., Auerbach, E. J., Bijsterbosch, J., Douaud, G., … Glasser, M. F. (2013). Resting-state fMRI in the human connectome project. *NeuroImage*, *80*, 144–168. https://doi.org/10.1016/j.neuroimage.2013.05.039

Smits, T., Aarnoudse, J., Geerdink, J., & Zijlstra, W. (1987). Hyperventilation-induced changes in periodic oscillations in forehead skin blood flow measured by laser Doppler flowmetry. *International Journal of Microcirculation, Clinical Experimental*, *6*(2), 149–159.

Stöcker, T., Schneider, F., Klein, M., Habel, U., Kellermann, T., Zilles, K., & Shah, N. J. (2005). Automated quality assurance routines for fMRI data applied to a multicenter study. *Human Brain Mapping*, *25*(2), 237–246. https://doi.org/10.1002/hbm.20096

Thayer, J. F., Åhs, F., Fredrikson, M., Sollers, J. J., III, & Wager, T. D. (2012). A meta-analysis of heart rate variability and neuroimaging studies: Implications for heart rate variability as a marker of stress and health. *Neuroscience Biobehavioral Reviews*, *36*(2), 747–756. https://doi.org/10.1016/j.neubiorev.2011.11.009

Thayer, J. F., & Lane, R. D. (2009). Claude Bernard and the heart–brain connection: Further elaboration of a model of neurovisceral integration. *Neuroscience & Biobehavioral Reviews*, *33*(2), 81–88. https://doi.org/10.1016/j.neubiorev.2008.08.004

Tokgözoglu, S. L., Batur, M. K., Topçuoglu, M. A., Saribas, O., Kes, S., & Oto, A. (1999). Effects of stroke localization on cardiac autonomic balance and sudden death. *Stroke*, *30*(7), 1307–1311. https://doi.org/10.1161/01.STR.30.7.1307

Toledo, E., Akselrod, S., Pinhas, I., & Aravot, D. (2002). Does synchronization reflect a true interaction in the cardiorespiratory system? *Medical Engineering Physics*, *24*(1), 45–52. https://doi.org/10.1016/s1350-4533(01)00114-x

Tong, Y., Hocke, L. M., & Frederick, B. B. (2019). Low frequency systemic hemodynamic "noise" in resting state BOLD fMRI: Characteristics, causes, implications, mitigation strategies, and applications. *Frontiers in Neuroscience*, *13*, 787. https://doi.org/10.3389/fnins.2019.00787

Veltman, J., & Gaillard, A. (1996). Physiological indices of workload in a simulated flight task. *Biological Psychology*, *42*(3), 323–342. https://doi.org/10.1016/0301-0511(95)05165-1

Weber, R., Behr, K.-M., Tamborini, R., Ritterfeld, U., & Mathiak, K. (2009). What do we really know about first-person-shooter games? An event-related, high-resolution content analysis. *Journal of Computer-Mediated Communication*, *14*(4), 1016–1037. https://doi.org/10.1111/j.1083-6101.2009.01479.x

Weiskopf, N., Veit, R., Erb, M., Mathiak, K., Grodd, W., Goebel, R., & Birbaumer, N. (2003). Physiological self-regulation of regional brain activity using real-time functional magnetic resonance imaging (fMRI): Methodology and exemplary data. *NeuroImage*, *19*(3), 577–586. https://doi.org/10.1016/S1053-8119(03)00145-9

Wiebking, C., de Greck, M., Duncan, N. W., Tempelmann, C., Bajbouj, M., & Northoff, G. (2015). Interoception in insula subregions as a possible state marker for depression—An exploratory fMRI study investigating healthy, depressed and remitted participants. *Frontiers in Behavioral Neuroscience*, *9*, 82. https://doi.org/10.3389/fnbeh.2015.00082

Williams, J. R. (2008). The Declaration of Helsinki and public health. *Bulletin of the World Health Organization*, *86*, 650–652.

Wong, S. W., Massé, N., Kimmerly, D. S., Menon, R. S., & Shoemaker, J. K. (2007). Ventral medial prefrontal cortex and cardiovagal control in conscious humans. *NeuroImage*, *35*(2), 698–708. https://doi.org/10.1016/j.neuroimage.2006.12.027

Yücel, M. A., Selb, J., Aasted, C. M., Lin, P. Y., Borsook, D., Becerra, L., & Boas, D. A. (2016). Mayer waves reduce the accuracy of estimated hemodynamic response functions in functional near-infrared spectroscopy. *Biomedical Optics Express*, *7*(8), 3078–3088. https://doi.org/10.1364/BOE.7.003078

Zamoscik, V. E., Schmidt, S. N. L., Gerchen, M. F., Samsouris, C., Timm, C., Kuehner, C., & Kirsch, P. (2018). Respiration pattern variability and related default mode network connectivity are altered in remitted depression. *Psychological Medicine*, *48*(14), 2364–2374. https://doi.org/10.1017/S0033291717003890

Ziege, S., Schmid-Schönbein, H., Grebe, R., & Martin, E. (1997). Long-term registration of cutaneous microcirculation during general anesthesia. *International Journal of Microcirculation*, *17*(6), 385–394. https://doi.org/10.1159/000179254

Zweerings, J., Hummel, B., Keller, M., Zvyagintsev, M., Schneider, F., Klasen, M., & Mathiak, K. (2019). Neurofeedback of core language network nodes modulates connectivity with the default-mode network: A double-blind fMRI neurofeedback study on auditory verbal hallucinations. *NeuroImage*, *189*, 533–542. https://doi.org/10.1016/j.neuroimage.2019.01.058

How to cite this article: Keller M, Pelz H, Perlitz V, et al. Neural correlates of fluctuations in the intermediate band for heart rate and respiration are related to interoceptive perception. *Psychophysiology*. 2020;57:e13594. https://doi.org/10.1111/psyp.13594

APPENDIX A

A.1 | FFT power spectrum (Welch's periodogram) of cardiac (blue) and respiratory (green) data

FFT power spectrum for RS fMRI across all participants showing mean power (line) and standard deviation (shadow). Peak power reflected by large standard deviation and mean can be seen within the LF band (0.05–0.12 Hz), the IM band (0.12–0.18 Hz), and the HF band (0.18–0.4 Hz; especially around 0.25 Hz, related to mean respiration frequency).

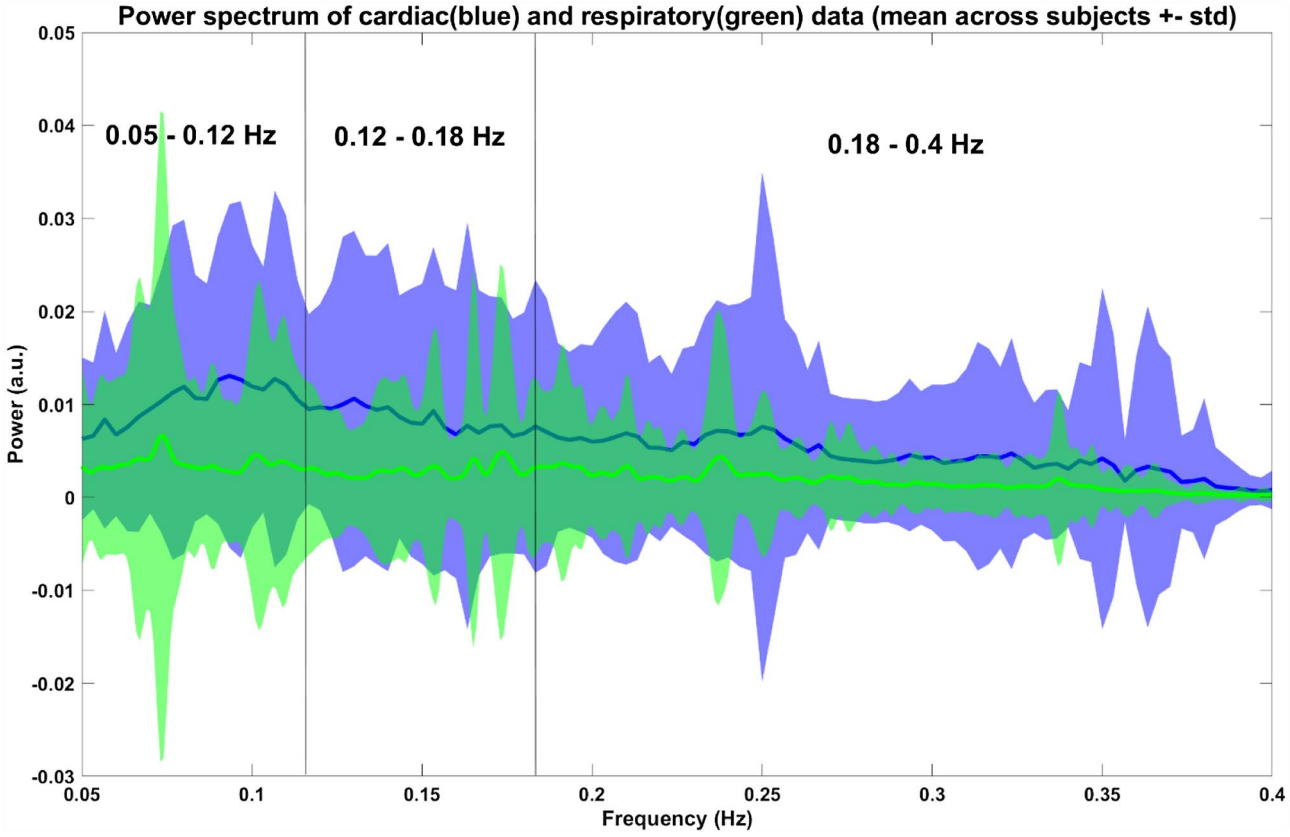

APPENDIX B

B.1 | Whole brain activation maps of LF and HF bands

Neural correlates of variability in cardiac and respiratory data for LF (0.05–0.12 Hz) and HF (0.18–0.4 Hz) bands. (Left panel) HRV in the LF band was negatively correlated with the BOLD response in the left and right postcentral gyrus (cold colors). HF band power was associated with activation (positive correlation indicated by warm colors) in core autonomic regulation areas (anterior insula, MCC, supramarginal/angular gyrus). (Right panel) No significant correlation emerged for LF respiratory data. HF band power was associated with the strongest BOLD activation which was found in DMN areas such as PCC/precuneus, angular gyri, and middle prefrontal cortex. All maps are corrected at FWE-cluster level $p < .05$ (after voxel level threshold $p < .001$).

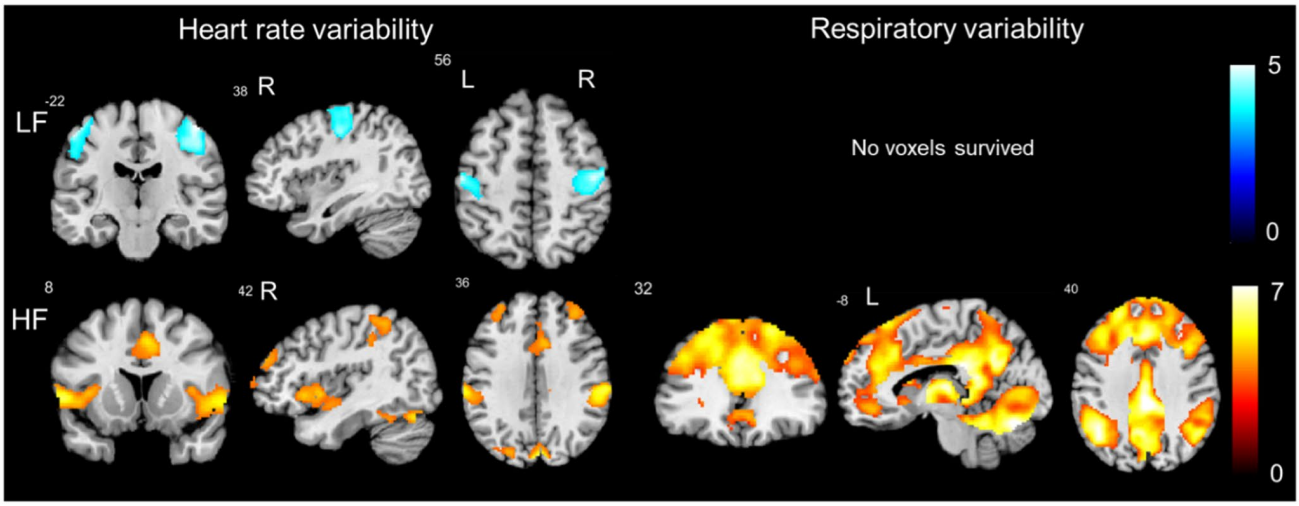

B.2 | Whole brain GLM results of the cardiac and respiratory LF and HF bands

The low frequency components of cardiac data were associated with deactivations in the pre- and postcentral gyri whereas BOLD activation related to LF respiratory signal did not survive the threshold for correction. However, the ROI analysis indicated that the respiratory LF band was also related to deactivations in widespread areas. This is in line with previous research (e.g., Critchley et al., 2002). As hypothesized, the HF-HRV was associated with activations in core ANS regulation areas, encompassing the insula, MCC, and supramarginal/angular gyrus, but also the precuneus, inferior frontal gyrus and cerebellum. Respiratory HF power recruited brain areas commonly associated with the default mode network (DMN), including the medial prefrontal cortex, PCC, precuneus, inferior parietal lobules, thalamus, and cerebellar vermis. These maps showed overlap with the IM band of HRV in PCC, precuneus, MCC, and cerebellar vermis (Appendix B.5).

B.3 | BOLD correlates of heart rate variability for LF and HF components

HRV-LF (negative)	MNI coordinates [mm]				
Location	*x*	*y*	*z*	Volume [voxel]	Peak *t*-value
Postcentral_R	46	−24	64	923	4.573
Postcentral_L	−48	−24	62	515	4.479
HRV-HF (positive)	MNI coordinates [mm]				
Location	*x*	*y*	*z*	Volume [voxel]	Peak *t*-value
Precuneus_R	6	−62	68	5,396	6.034
SupraMarginal_R	60	−28	30	5,396	5.401
Cerebelum_Crus1_R	12	−86	−18	3,022	5.348
Temporal_Mid_L	−60	−62	−2	3,022	5.313
Frontal_Mid_2_L	−46	44	16	729	5.000
Frontal_Inf_Tri_R	54	40	4	1,263	4.985
Frontal_Inf_Oper_L	−56	6	6	1,081	4.973
Rolandic_Oper_R	58	14	0	1,137	4.850
SupraMarginal_L	−64	−32	32	831	4.682
Postcentral_L	−28	−40	74	831	3.968
Supp_Motor_Area_R	4	6	46	806	4.327

Clusters reported at $p < .05$ FWE-corrected ($p < .001$ voxelwise threshold).

B.4 | Bold correlates of respiratory variability for LF and HF components

Resp-LF and Resp-HF					
	No voxels survived correction				
Resp_HF (positive)	MNI coordinates [mm]				
Location	*x*	*y*	*z*	Volume [voxel]	Peak *t*-value
Vermis_6	−2	−76	−14	44,911	7.902
Angular_L	−40	−66	44	44,911	7.675
Cingulate_Mid_R	2	−36	40	44,911	7.602
Cingulate_Post_L	−2	−48	18	44,911	7.257
Cingulate_Post_L	−2	−34	28	44,911	7.238
Cingulate_Mid_L	−2	−28	34	44,911	7.106
Angular_R	44	−64	44	2,280	6.340
Angular_R	38	−64	50	2,280	6.238
Parietal_Inf_R	46	−52	50	2,280	5.827
SupraMarginal_R	44	−44	30	2,280	5.162
Angular_R	38	−56	36	2,280	5.107
SupraMarginal_R	46	−38	30	2,280	4.368

Clusters reported at $p < .05$ FWE-corrected ($p < .001$ voxelwise threshold).

B.5 | Conjunction map of cardiac IM band (red) and respiratory HF band (green)

Overlap of the two statistical maps is shown in yellow. Maps show overlap in default mode network areas (PCC/precuneus) as well as cerebellum. All maps are corrected at FWE-cluster level $p < .05$ (after voxel level threshold $p < .001$).

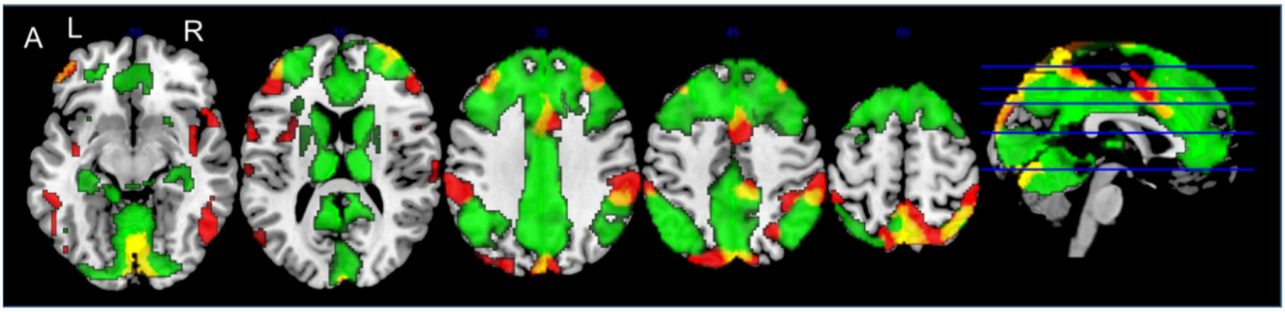

APPENDIX C

C.1 | Discussion of LF and HF bands results

In line with the literature, the LF band was related to negative correlations throughout the brain. For instance, Critchley et al. (2002) showed in an electrodermal activity (EDA; a measure related to sympathetic activity) biofeedback study that the level of EDA correlated negatively with activations in the ACC, dorsolateral prefrontal cortex, basal ganglia, somatosensory cortex, thalamus, and pons. Furthermore, these areas are also related to interoceptive awareness (Craig & Craig, 2009) which may suggest that the LF component is possibly associated with a shift from internal processes to the external environment. Deactivation of the interoceptive network may be an adaptive process related to general arousal. The LF band was also associated with deactivations in the amygdala. In the framework of sympathetic predominance, this finding seems counterintuitive. According to the neurovisceral integration model (Thayer & Lane, 2009), prefrontal inhibition related to sympathetic activation leads to a disinhibition of the amygdala. Hence, if the LF band is related to sympathetic activation, it should be associated with higher activation in the amygdala. However, the LF band may be difficult to interpret in terms of ANS activity as it has been shown to be modulated by both, parasympathetic and sympathetic influences (e.g., Reyes del Paso et al., 2013).

HF-HRV correlates were found in core ANS regulation areas (Beissner et al., 2013). The activations observed during RS fMRI were also consistent with the neurovisceral integration model which posits that HF-HRV is related to activation in executive control areas (Thayer & Lane, 2009). To our knowledge, the neural correlates of different frequency bands of respiratory power have not been investigated thus far. However, the widespread activation in the respiratory HF band is in line with the model of respiratory control proposed by Evans (2010) who suggests an interplay of respiratory motor areas (SMA, premotor cortex, thalamus, basal ganglia, brainstem, and cerebellum) and interoceptive integration areas (cingulate cortex, insula, and amygdala).